

## NEW CERES RESULTS

A. MARÍN for the CERES COLLABORATION

*Gesellschaft für Schwerionenforschung (GSI), Planckstr. 1, 64291 Darmstadt, Germany*

During 1999 the CERES experiment upgraded by the new TPC was taking data from semi-central Pb+Au collisions at 40 AGeV. The analysis of the di-electron spectra shows an enhancement in the low mass region of at least the same magnitude as previously observed at full SPS energy. The results are compared to model calculations with and without medium modifications of the vector mesons. The addition of the radial TPC gives more possibilities to study hadronic observables. The results obtained for the midrapidity  $\Lambda$  yield and the  $\bar{\Lambda}/\Lambda$  ratio are compared to the existing systematics.

### 1 Introduction

The CERES/NA45 experiment at CERN SPS is dedicated to the measurement of low-mass  $e^+e^-$  pairs<sup>1</sup> in ultrarelativistic heavy-ion collisions. QCD calculations have predicted a transition from ordinary hadronic matter into a plasma of deconfined quarks and gluons at high energy density. Dileptons, which have negligible final state interactions, represent a more suitable probe than hadrons for the study of this new state of matter. CERES has observed an enhanced dilepton production in the invariant mass region  $m_{e^+e^-} > 0.2$  GeV/ $c^2$  in Pb+Au at 158 AGeV and in S+Au at 200 AGeV<sup>1</sup> compared to the contribution from known hadronic sources. The enhancement is not present on p-induced reactions<sup>2</sup>. Pion annihilation has been pointed out as a possible mechanism for additional  $e^+e^-$  production but the shape of the experimental spectra cannot be explained without introducing medium modifications of vector mesons, particularly of the  $\rho$ . The transition from normal hadronic matter to a state in which chiral symmetry is restored is believed to be influenced by baryon density more strongly than by temperature<sup>3</sup>. CERES was running during 1999 at 40 AGeV, thus, providing a second measurement at very different values of  $\rho$  and T compared to 158 AGeV<sup>4</sup>. In addition hydrodynamical calculations showed that the softest point is reached in heavy ion collisions at around 30 AGeV<sup>5</sup>. Measuring at lower energies could be a strategy to search for the QCD phase transition.

We will focus in this article on the results from 1999 data taking concerning dileptons<sup>6,7</sup> and  $\Lambda$ <sup>8</sup> hyperons. A total of about  $8 \cdot 10^6$  events with 30% centrality were recorded. Due to readout problems in part of the detector this data set is limited in terms of statistics and momentum resolution.

### 2 Experimental Setup

The CERES experiment is optimized to measure low mass electron pairs close to midrapidity ( $2.1 < \eta < 2.6$ ) with full azimuthal coverage. In order to improve the mass resolution to  $\delta m/m < 2\%$  the CERES experiment was upgraded in 1998 with the addition of a cylindrical radial drift

TPC and a new magnet system<sup>9</sup>. A silicon telescope, composed of two silicon drift chambers (SDD) positioned at 10 cm and 13.8 cm behind a segmented Au target, provides a precise vertex reconstruction and angle measurement for charged particles. Two Ring Imaging CHerenkov (RICH) detectors operated at a high threshold ( $\gamma_{th}=32$ ) are used for electron identification in a huge hadronic background. The new radial drift TPC positioned downstream from the existing spectrometer has an active length of 2 m and an outer diameter of 2.6 m. It is operated inside a variable magnetic field with a maximal radial component of 0.5 T providing the measurement of up to 20 space points for each charged particle track. This is sufficient for the momentum determination and additional particle ID via  $dE/dx$ . As particle ID and momentum measurement are separated in the upgraded apparatus, the two RICH detectors can be used in a combined mode, resulting in an improved electron efficiency (from 0.70 in 1995/96 to 0.94 in 1999) and improved rejection power. Moreover, the addition of the radial TPC gives wider possibilities to study hadronic observables.

### 3 Electron analysis

Electrons are identified by the ring pattern detected in the RICH detectors. An electron track is constructed by matching RICH rings to the track segments identified in the SDD and TPC. Invariant mass is calculated by pairing oppositely charged electron tracks. Although the RICH detectors reject 95% of all hadrons and the total detector material is kept as low as  $X/X_0=1\%$  the main problem of an electron analysis is the combinatorial background due to photons from conversions and  $\pi^0$  Dalitz decays and to remaining hadrons.

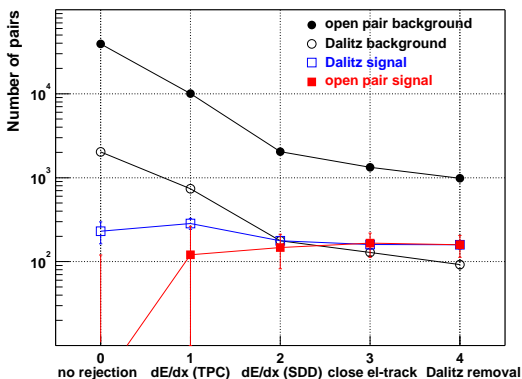


Figure 1: Evolution of the total number of pairs after various rejection steps, shown for the open pair signal ( $m_{ee} > 0.2 \text{ GeV}/c^2$ ), open pair background ( $m_{ee} > 0.2 \text{ GeV}/c^2$ ), Dalitz signal ( $m_{ee} < 0.1 \text{ GeV}/c^2$ ) and Dalitz background ( $m_{ee} < 0.1 \text{ GeV}/c^2$ ).

A few experimental cuts applied in the analysis provide a rejection factor larger than 100 with efficiency losses for open pairs less than a factor 2 (extracted from Dalitz signal losses), as illustrated in Fig. 1. Only electron tracks with transverse momenta  $p_t > 0.2 \text{ GeV}/c$  and with an opening angle  $\theta_{e^+e^-} > 35 \text{ mrad}$  are taken (Fig. 1, cut 0). Additional electron identification and pion rejection is achieved by a cut in  $dE/dx$  in the TPC as a function of the momentum (Fig. 1, cut 1). Conversions and Dalitz pairs with too small opening angle to create two separate RICH rings produce a double energy loss within small angular region in the SDD and can be removed by applying an upper cut in SDD  $dE/dx$  (Fig. 1, cut 2). Due to the incomplete azimuthal readout of the TPC in 99 data set electron tracks that have a second SDD-RICH candidate within 70 mrad are also rejected (Fig. 1, cut 3). Positively identified Dalitz pairs are excluded for further combinatorics (Fig. 1, cut 4). The final dilepton spectrum (Fig. 2) is obtained by subtracting the like-sign pairs from the unlike-sign pairs as  $N_{e^+e^-} - 2(N_{e^+e^+} \cdot N_{e^-e^-})^{1/2}$ .

A total of  $185 \pm 48$  open pairs for  $m_{e^+e^-} > 0.2 \text{ GeV}/c^2$  with a signal to background ratio of  $S/B = 1/6$  is obtained from the analysis of 40 AGeV data. Comparing to the hadronic decay cocktail an enhancement factor of  $5.1 \pm 1.3$  (stat.) is obtained. The pair  $p_t$  distributions for two

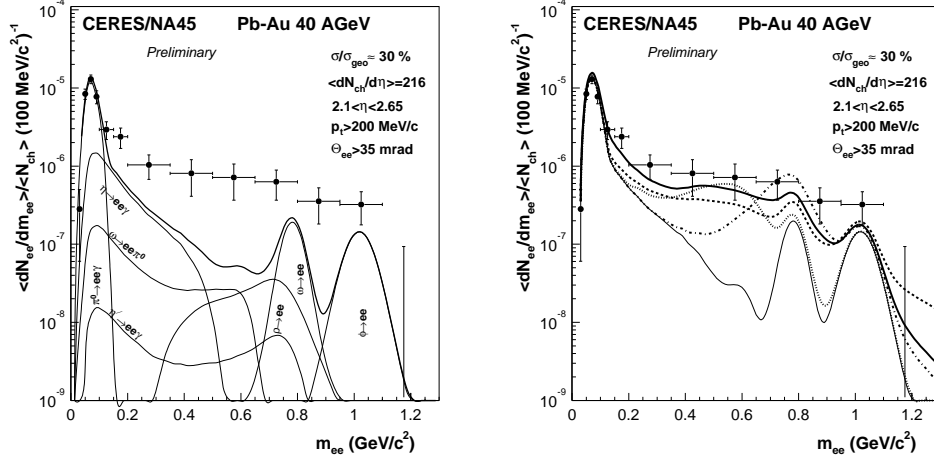


Figure 2: Invariant mass spectrum of  $e^+e^-$  pairs at 40 AGeV. Left: Comparison to the expectations from known hadronic sources in heavy ion collisions (“decay cocktail”). Right: Comparison of the data to model calculations, based on  $\pi^+\pi^-$  annihilation with an unmodified  $\rho$  (dashed-dotted), a dropping  $\rho$  mass (dotted) and broadening of the  $\rho$  spectral function (thick solid). Also shown is the hadronic cocktail without  $\rho$  (solid). The lowest order pQCD rate calculation (dashed).

regions of mass  $m_{e^+e^-} < 0.2 \text{ GeV}/c^2$  and  $m_{e^+e^-} > 0.2 \text{ GeV}/c^2$  shows that the enhancement is localized at low  $p_t$  in agreement with the observation at 158 AGeV. From the comparison to theory<sup>10</sup> (Fig. 2) one concludes that strong medium modifications of the intermediate  $\rho$  are needed to explain the data but the accuracy of data does not allow to distinguish between different scenarios,  $\rho$  scaling reducing the mass or broadening of the  $\rho$  spectral function. The enhancement is consistent or even larger than the one observed at 158 AGeV showing that baryons play the dominant role in the medium modifications of the  $\rho$ .

#### 4 $\Lambda$ production

The addition of the radial TPC gives more possibilities to study hadronic observables in the CERES experiment. For example, it allows a systematic investigation of the  $\Lambda$  hyperon at midrapidity. The  $\Lambda$  hyperon is reconstructed by the invariant mass of positive and negative particles in one event<sup>8</sup>. Only the information of the TPC and the SDD detector are used in this analysis. Positive particles are taken in the transverse momentum range  $0.5 < p_t < 2.0 \text{ GeV}/c$  and negatives in the range  $0.25 < p_t < 0.6 \text{ GeV}/c$ . The final  $\Lambda$  acceptance is  $0.9 < p_t < 2.5 \text{ GeV}/c$  and  $2.0 < y < 2.4$ . A cut on the Armenteros Podolanski plot of 10-120 MeV/c in  $p_t^+$  and  $\alpha < 0.65$  is applied. Three analysis methods were used: first, only TPC information is required. Second, TPC tracks should not have a matched track in the SDD, in that way only  $\Lambda$ 's decaying at least 13 cm after the vertex are detected. Third, after reconstructing the decay point an additional cut of 50 cm in the decay point is applied. The invariant mass spectra for the three different methods assuming positives to be protons and negatives to be pions is shown in Fig. 3 (left). Although one can notice a loss of signal, a large improvement in signal to background is obtained as successive cuts are introduced. After subtraction of the combinatorial background the  $\Lambda$  signal is obtained at a mass of  $m_\Lambda = 1.117 \pm 0.001 \text{ GeV}/c^2$  close to the PDG value. The width  $\sigma_\Lambda = 11.2 \pm 0.4 \text{ MeV}/c^2$  is larger than that expected from the design momentum resolution due to the incomplete calibration process. As consistency check the number of  $\Lambda$ 's as a function of the decay point is fitted to an exponential function giving a  $c\tau_0$  of  $(8.1 \pm 0.5) \text{ cm}$ , in agreement with the tabulated value of 7.89 cm. Transverse momentum distributions are depicted in Fig. 3 (right). An inverse slope parameter  $T$  of  $273 \pm 20 \text{ MeV}$  is obtained from a fit to an exponential

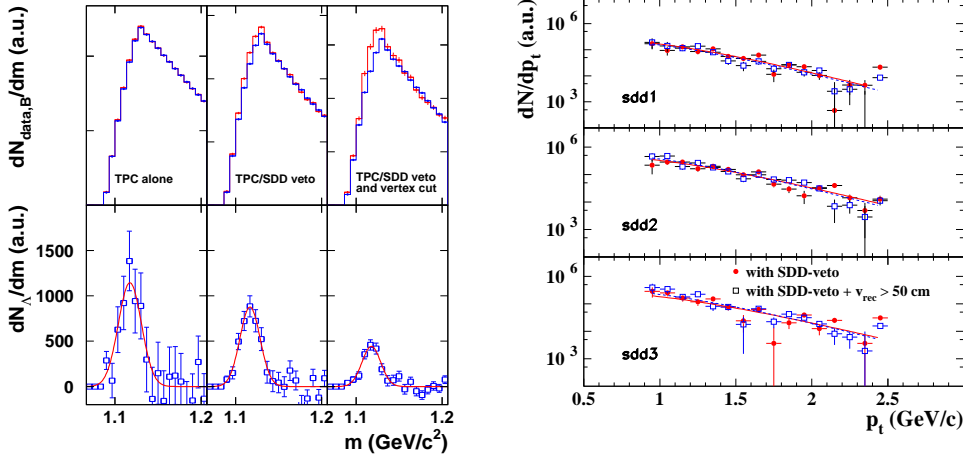


Figure 3: Left: Invariant mass of positive and negative particles (dashed line) and combinatorial background (solid line) for the three analysis methods. In the bottom is shown the signal after background subtraction. Right: Transverse momentum spectra for  $\Lambda$  shown separately for two different analysis methods and for the three centrality classes in the rapidity region  $2 < y_\Lambda < 2.4$ . All spectra are acceptance corrected but not normalized to the number of events.

function  $dN/p_t dp_t \propto \exp(-m_t/T)$ , slightly increasing with centrality.

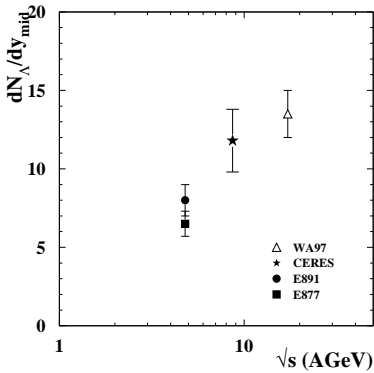


Figure 4:  $dN_\Lambda/dy_{mid}$  as a function of beam energy  $\sqrt{s}$ .

A midrapidity density of  $dN_\Lambda/dy_{mid} = 11.8 \pm 2.0$  is obtained by extrapolating the transverse momentum spectra to  $p_t=0$  using the fitted function. In addition a ratio of  $\bar{\Lambda}/\Lambda = 0.024 \pm 0.010$  has been obtained, in agreement with the result reported by NA57<sup>11</sup>.

When comparing the midrapidity  $\Lambda$  yield (Fig. 4) and  $\bar{\Lambda}/\Lambda$  ratio<sup>8</sup> to the results at AGS<sup>12,13</sup> and full SPS<sup>14</sup> one observes a monotonic rising behaviour with increasing beam energy.

## References

1. G. Agakichiev *et al.* CERES Collaboration *Phys. Rev. Lett.* **75**, 1272 (1995); *Phys. Lett. B* **422**, 405 (1998); 1999 *Nucl. Phys. A* **661**, 23c (1999).
2. G. Agakichiev *et al.* *Eur. Phys. J C* **4**, 231 (1998).
3. S. Klimt, M. Lutz and W. Weise *Phys. Lett. B* **249**, 386 (1990).
4. G.E. Brown and M. Rho *Phys. Rev. Lett.* **66**, 2720 (1991); T. Hatsuda and S. Lee *Phys. Rev. C* **46**, R34 (1992); M. Herrmann, B. Friman, W. Nörenberg *Nucl. Phys. A* **560**, 411 (1993); K.Haglin, *Nucl. Phys. A* **584**, 719 (1995).
5. C.M. Hung and E.V. Shuryak *Phys. Rev. Lett.* **75(22)**, 4003 (1995).
6. S. Damjanović and K. Filimonov. Proc. of Int. Europhys. Conf. in HEP, Budapest, 2001.
7. H. Appelshäuser for the CERES Collaboration *Nucl. Phys. A* **698**, 253c (2002).
8. W. Schmitz for the CERES Collaboration SQM01 (to be published) *J. Phys. G*, ().
9. A. Marín for the CERES Collaboration *Nucl. Phys. A* **661**, 673c (1999).
10. R. Rapp. Private communication.
11. N. Carrer for the NA57 Collaboration *Nucl. Phys. A* **698**, 118c (2002).
12. S. Ahmad *et al.* E891 Collaboration *Phys. Lett. B* **382**, 35 (1996).
13. K. Filimonov for the E877 Collaboration *Nucl. Phys. A* **661**, 198c (1999).
14. F. Antinori *et al.* WA97 Collaboration *Eur. Phys. J C* **11**, 79 (1999).